1966

A crystallographic study of the $PbZrO_3$-$PbTiO_3$-$BiFeO_3$ ternary system.

Dannie R. Clarida

Department:

A CRYSTALLOGRAPHIC STUDY OF THE $PbZrO_3$-$PbTiO_3$-$BiFeO_3$ TERNARY SYSTEM

BY

DANNIE RAY CLARIDA

A

THESIS

submitted to the faculty of

THE UNIVERSITY OF MISSOURI AT ROLLA

in partial fulfillment of the requirements for the

Degree of

MASTER OF SCIENCE IN CHEMICAL ENGINEERING

Rolla, Missouri

1966

Approved by

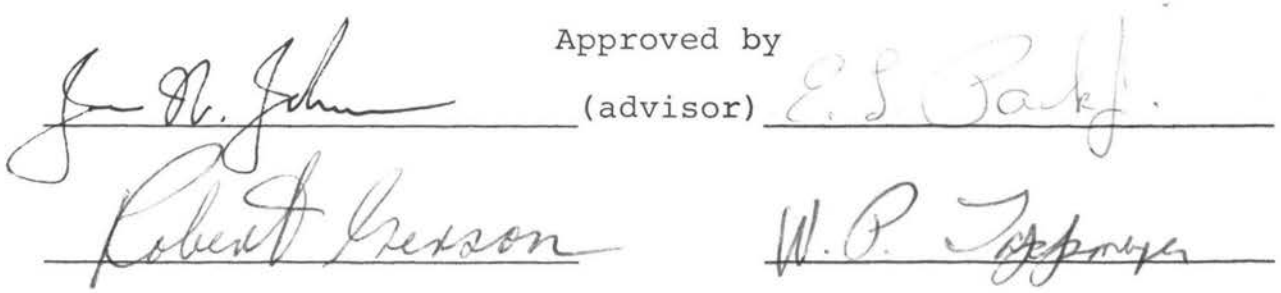

ABSTRACT

The purpose of this investigation was to conduct a crystallographic study of the $PbZrO_3$-$PbTiO_3$-$BiFeO_3$ ternary system, where all three components are perovskites. Lead zirconate is antiferroelectric, lead titanate is ferroelectric, and bismuth ferrate is thought to be ferroelectric. X-ray diffraction analysis was employed to determine the crystallographic structure and lattice parameters.

A tetragonal region was found to exist in the area of high $PbTiO_3$ content. A rhombohedral region occurred in the remainder of the system with high $BiFeO_3$ and $PbZrO_3$ content, except for an orthorhombic envelope along the $PbZrO_3$-$BiFeO_3$ side of the diagram up to approximately 70 per cent $BiFeO_3$. The phase boundaries in the system had a phase width, rather than being distinct lines.

The addition of $PbZrO_3$ to the binary $PbTiO_3$-$BiFeO_3$ suppresses the normally increasing c/a ratio which occurs as the $BiFeO_3$ content is increased. At 50 $PbZrO_3$:50 $PbTiO_3$, the addition of $BiFeO_3$ decreases this ratio.

The orthorhombic region near the $PbZrO_3$-$BiFeO_3$ binary was indexed using a multiple-cell orthorhombic structure. All three lattice parameters decreased with additions of $BiFeO_3$.

High resolution conditions on the diffractometer were required to determine the peak splitting on most of

the rhombohedral x-ray patterns. The rhombohedral distortion increased and the "a" parameter decreased with increasing $BiFeO_3$ content.

The dielectric constant and Curie point were determined for various ratios of $BiFeO_3$ and 50 $PbZrO_3$:50 $PbTiO_3$. The Curie point was found to be 380 and 400°C for 20 and 30 per cent $BiFeO_3$, respectively. For 20 per cent $BiFeO_3$, a dielectric constant of 685 was ascertained. The present study finds significantly higher electrical properties than those reported previously.

ACKNOWLEDGEMENTS

The author wishes to thank Dr. William J. James, Director of the Graduate Center for Materials Research, and Dr. Robert Gerson, Professor of Physics, for their guidance, support, and encouragement during the course of this investigation. He also wishes to thank Dr. James W. Johnson, Associate Professor of Chemical Engineering, for his assistance in the writing of this thesis.

The author is also grateful for the financial aid received from the National Science Foundation in the form of a traineeship and from the Atomic Energy Commission in supporting the project of which this investigation is a part.

TABLE OF CONTENTS

LIST OF FIGURES

LIST OF TABLES

I. INTRODUCTION

The purpose of this investigation was to conduct a crystallographic study of the $PbZrO_3$-$PbTiO_3$-$BiFeO_3$ pseudo-ternary system. This was done by determining the crystallographic structure and lattice parameters of various stoichiometric mixtures of the components by means of x-ray diffraction patterns. The work was undertaken mainly to establish a basis for study of the electrical and magnetic properties of the system.

The ferroelectric properties of $BiFeO_3$, $PbZrO_3$, and $PbTiO_3$, as well as other related materials, have been of considerable interest during the last few years. $PbZrO_3$ is antiferroelectric, while $PbTiO_3$ is ferroelectric. Both the $PbZrO_3$-$BiFeO_3$ [1] and $PbTiO_3$-$BiFeO_3$ [2] pseudo-binary systems have been investigated, and it was reported that $BiFeO_3$ was a ferroelectric with a Curie point between 800 and 900°C. This was found by extrapolating the Curie point of solid solutions to 100 per cent $BiFeO_3$, since direct measurement was prevented by the high conductivity of pure $BiFeO_3$. The $PbZrO_3$-$PbTiO_3$ pseudo-binary system has been studied, [3-6] resulting in the finding of marked piezoelectric properties, especially in the area of the rhombohedral-tetragonal transition region.

As a result of the limited amount of work that has been done on the pseudo-ternary system, it was reported that addition of $BiFeO_3$ to $PbZrO_3$-$PbTiO_3$ solid solutions close to

the rhombohedral-tetragonal transition region improved the piezoelectric properties and simplified the technique of preparation.[7] Therefore, it was decided that it would be of interest to combine the three pseudo-binary systems ($PbZrO_3$-$PbTiO_3$, $PbTiO_3$-$BiFeO_3$, and $PbZrO_3$-$BiFeO_3$) to form a pseudo-ternary system and determine whether solid solubility existed over the entire system. Should this be true, the resulting materials might have useful electrical and magnetic properties. In reporting the work on the $PbTiO_3$-$BiFeO_3$ system, Fedulov, et al.[2] mentioned that, "It would be expedient (with the object of obtaining high temperature piezoelectric materials) to introduce substances [$PbZrO_3$] which would decrease the conductivity of the specimens but improve the polarization conditions."

Thus, the specific objectives of this study were: (1) a determination of the phase diagram of the $PbZrO_3$-$PbTiO_3$-$BiFeO_3$ ternary system, and (2) use of this information to infer properties of $BiFeO_3$.

II. LITERATURE REVIEW

The pseudo-ternary system ($PbZrO_3$-$PbTiO_3$-$BiFeO_3$) that was investigated was found by putting together the three pseudo-binary systems, ($PbZrO_3$-$PbTiO_3$, $PbZrO_3$-$BiFeO_3$, and $PbTiO_3$-$BiFeO_3$). Therefore, each of these pseudo-binary systems will be reviewed in addition to the limited amount of work reported on the pseudo-ternary system. Hereafter, the pseudo designation of the binary and ternary systems will be dropped for clarity and ease of reference, realizing that the systems are actually composed of the respective oxides.

A. $PbZrO_3$-$PbTiO_3$ Binary System

Since $PbTiO_3$ has the highest known Curie temperature among perovskite-type ferroelectrics, almost any substitution for Pb or Ti which will form a perovskite-type lattice will lower the Curie point. This system was considered for investigation mainly to see the results of forming a solid solution from ferroelectric $PbTiO_3$ and antiferroelectric $PbZrO_3$.

A ferroelectric rhombohedral phase was found to exist between the orthorhombic and tetragonal phases characteristic of $PbZrO_3$ and $PbTiO_3$, respectively. This ferroelectric phase occurred between the limits of approximately 5 to 42 per cent (molar) $PbTiO_3$.[5] A very large piezoelectric modulus was reported for solid solutions close to the rhombohedral-tetragonal phase boundary.[6] The Curie point

was about 230°C for 100 per cent $PbZrO_3$ and dropped slightly until the rhombohedral region was reached. It then began to rise until a value of approximately 480°C was reached for 100 per cent $PbTiO_3$. [5]

B. $PbTiO_3$-$BiFeO_3$ Binary System

Fedulov, et al. [2] investigated this binary system and reported bismuth ferrate to be a ferroelectric with a Curie point of approximately 850°C. The existence of paramagnetic Fe^{+3} ions in $BiFeO_3$ gave grounds for belief that solid solutions based on $BiFeO_3$ would possess special magnetic properties. This was later proven correct by neutron diffraction [8] and direct magnetic measurements. [9,10]

The concentration limits of the two-phase region (rhombohedral-tetragonal) was also investigated by Fedulov, et al. [2], because of the probability of increased piezoelectric activity in this region. They reported the two-phase region to extend from 66 to 73 per cent (molar) $BiFeO_3$ and the tetragonal-rhombohedral transition to occur at approximately 70 per cent (weight) $BiFeO_3$. The c/a ratio for the tetragonal modification was found to increase with increasing percentages of $BiFeO_3$, although the volume of the unit cell remained essentially the same. The parameters of the unit cells within the two-phase region did not change. The "a" parameter of the rhombohedral unit cell decreased slightly as more $BiFeO_3$ was added beyond the transition region. All of the solid solutions containing various amounts of $BiFeO_3$ that were investigated for mag-

netic properties were found to be antiferromagnetics with weak ferromagnetism. An increase of $PbTiO_3$ resulted in a reduction of the Neél temperature. The Neél temperature dropped from 370°C in pure $BiFeO_3$ to 60°C in material containing 70 per cent (weight) $PbTiO_3$.

Another group [11] has confirmed the crystallographic results just mentioned. In addition, the tetragonal distortion was found to be very sensitive to thermal history. In an attempt to reproduce the results of Fedulov, et al.,[2] it was observed that the width of the transition region was approximately the same as reported, but it was shifted so that it existed from about 71 to 76 per cent (molar) $BiFeO_3$. When lower sintering temperatures were used (720 versus 1000°C), the two-phase region was extended over a compositional region that was about five times as great as that at high temperatures.

C. $PbZrO_3$-$BiFeO_3$ Binary System

This binary system has been investigated by various groups in the past; [12-14] however, most of them have had difficulty obtaining completely perovskite solid solutions. However, within the past year, some perovskitic solid solutions of this system with a minimum amount of contamination were prepared at the UMR Graduate Center for Materials Research. [15] The contamination was usually γ-Bi_2O_3, or Bi_2O_3-$2Fe_2O_3$. The ZrO_2 was most prevalent but its concentration did not exceed 3 per cent (molar) and was usually lower.

In addition to the known rhombohedral and orthorhombic phases of $BiFeO_3$, a third phase was found to exist in the region of about 80 to 30 per cent (molar) $PbZrO_3$. [15] This phase had a crystal structure of multiple-cell orthorhombic and appeared to be ferroelectric, as opposed to the antiferroelectric $PbZrO_3$. The ferroelectricity of this new phase was established by the nature of the non-linear behavior of the dielectric constant.

In a diagram of Curie point versus composition, there was a minimum (155°C) at the phase boundary between the two orthorhombic phases. Also, an extrapolation of the curve showed a Curie point of about 900°C for $BiFeO_3$, which gave evidence to the hypothesis that $BiFeO_3$ has ferroelectric properties. The ferroelectricity of this intermediate phase was also shown by the lowering of the small-signal dielectric constant on the application of a bias field. This was due primarily to the orientation of the ferroelectric domains with their polar axes parallel to the field, the polar axis being the direction of low dielectric constant.

D. $PbZrO_3$-$PbTiO_3$-$BiFeO_3$ Ternary System

The only work reported on this system was by Ikeda and Okano [7] in Japan. They investigated mainly the extension of the rhombohedral-tetragonal phase boundary of the $PbZrO_3$-$PbTiO_3$ binary system upon addition of $BiFeO_3$. Specimens were made near this boundary with up to 50 per cent (molar) $BiFeO_3$ in order to study possible piezo-

electric properties. The width of the investigated region was from 40 to 70 per cent $PbZrO_3$.

The ferroelectric Curie point was found to fall at first and then rise with increasing $BiFeO_3$ content, and to fall gradually with increasing $PbZrO_3$. In the ferroelectric materials, the dielectric constant increased according to the Curie-Weiss Law.

It was reported in this study that the addition of $BiFeO_3$ to $PbZrO_3$-$PbTiO_3$ solid solutions improves the piezoelectric properties, especially since it lowers the sintering temperature and increases the electromechanical coupling coefficient. However, these results are questionable because low density ceramics were used to determine the dielectric properties. They were not as good as the ones reported previously [6] for $PbZrO_3$-$PbTiO_3$ without additions of $BiFeO_3$.

The results of this investigation showed the rhombohedral-tetragonal phase boundary to extend from approximately 55 per cent (molar) $PbZrO_3$ on the $PbZrO_3$-$PbTiO_3$ side and across the vertical line (from 50 per cent $PbZrO_3$ to pure $BiFeO_3$) at approximately 35 per cent $BiFeO_3$ as it curved toward the $PbTiO_3$-$BiFeO_3$ side of the ternary diagram. The remainder of the phase boundary was not determined. Figure 1 shows the extent of the work that was reported at the start of the present investigation.

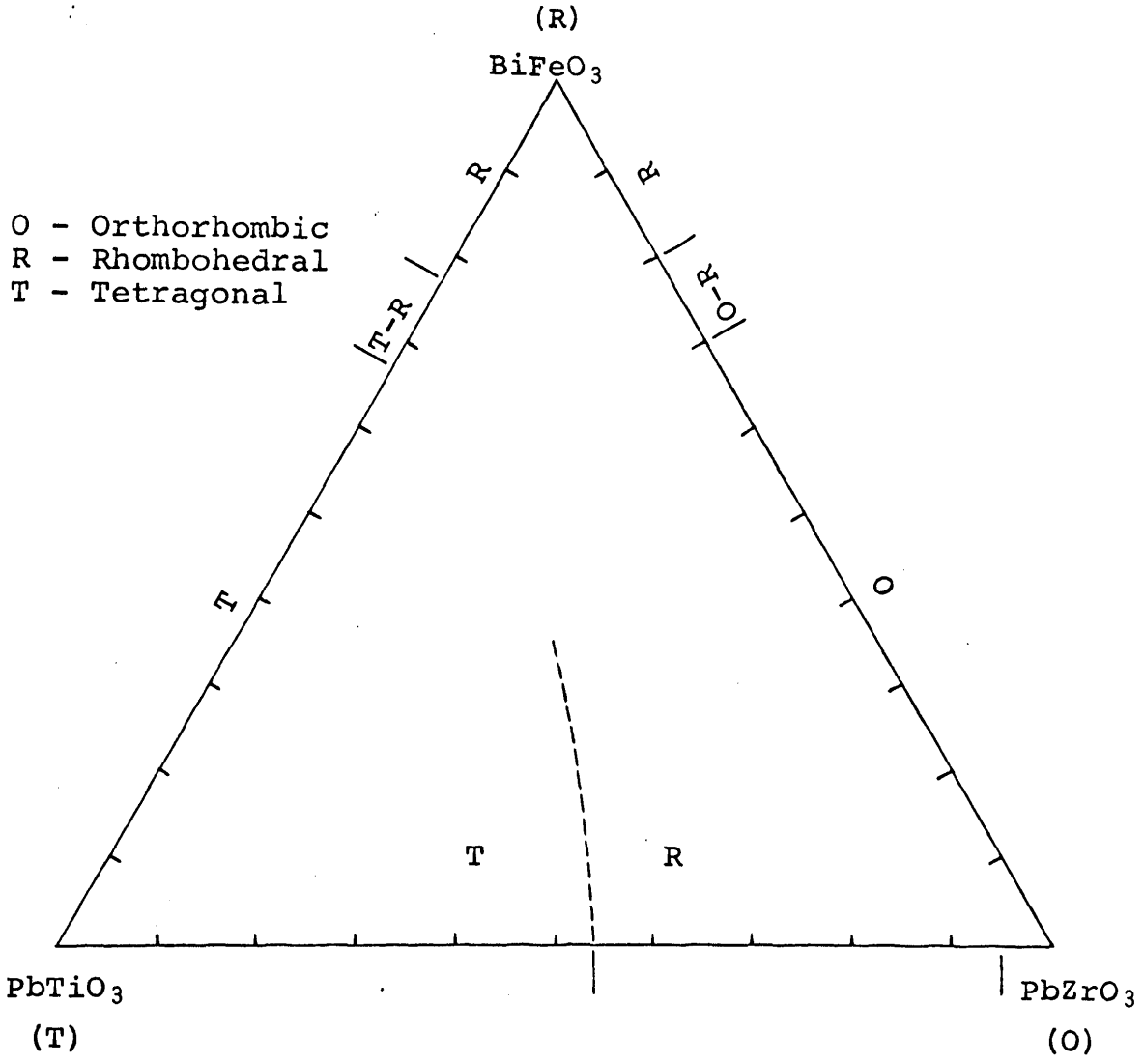

Figure 1. Sketch of previous work done on ternary system.

III. EXPERIMENTAL PROCEDURE

A. Materials

The materials used in the preparation of the various samples were PbO, ZrO_2, TiO_2, Bi_2O_3, and Fe_2O_3. The purity and manufacturer of each of these oxides are listed in Appendix A. Distilled water was used in the making and filtering of the ball milled samples.

B. Apparatus

The uses of the various apparatus will be described here, and a list of apparatus appears in Appendix B.

1. Analytical balance. A regular two pan balance and a single pan balance were both used in weighing the materials to make the samples. Each balance had a sensitivity of 1/10,000 gram.

2. Mortar and pestle. Three types of mortar and pestles were employed to mix and grind the samples before sintering and to grind the sintered samples in preparation for x-ray diffraction analysis. An agate and a porcelain mortar and pestle were both used before and after sintering. An alumina automatic mortar and pestle was utilized in the pre-sintering procedure of mixing the various samples. These mortars and pestles are described here in detail, because no contamination was found to occur from their use.

3. Ball mill. A ball mill was used in preparing large amounts of each of the three components of the ternary system. Various stoichiometric amounts of these components

were then used in making the samples for sintering.

The ball mill was constructed from a 250 ml plastic bottle that contained approximately 25 ceramic balls (0.4 inch dia.) and could be rotated at an inclined angle by a variable speed motor. Distilled water was added with the material to form a slurry. After rotating a few hours, the slurry was filtered with distilled water and dried in a drying oven. No contamination from the ball mill was found.

4. Crucible. A covered alumina (morganite) crucible, lined with platinum foil, was utilized to sinter the samples. This crucible was very dense and helped in curtailing any possible loss of Bi_2O_3 during sintering. The crucible was approximately 0.8 inch in diameter and 0.875 inches high.

5. Furnace. Two furnaces were used to sinter the samples. One was a platinum-wound resistance furnace with a maximum temperature limit of 1200°C, and the other was a Kanthal-wound resistance furnace with a maximum temperature limit of 1000°C. Both furnaces were equipped with automatic controls. The furnaces were calibrated periodically to insure correct temperatures. The Kanthal furnace was large enough to sinter two samples at the same time; whereas, the tube in the platinum furnace was only large enough for one crucible.

6. X-ray diffraction unit. Siemens and General Electric diffraction units were employed in making x-ray diffraction patterns of the sintered samples to determine

the crystallographic structure and lattice parameters. Copper Kα radiation, with a Ni filter, was used. This type was employed because of the good background with no fluorescence.

C. Preparation of Samples

1. Weighing of materials. There were two basic methods utilized in the weighing of materials for the various stoichiometric mixtures. One was to weigh out all of the oxides needed for a particular sample, and the other was to weigh out the necessary amounts of the three main components ($PbZrO_3$, $PbTiO_3$, and $BiFeO_3$), which had been prepared previously from the respective oxides. The method of weighing is designated in Appendix C. The equations used to determine the stoichiometric ratios were:

$$PbO + ZrO_2 \longrightarrow PbZrO_3 \quad (1)$$

$$PbO + TiO_2 \longrightarrow PbTiO_3 \quad (2)$$

$$Bi_2O_3 + Fe_2O_3 \longrightarrow 2BiFeO_3 \quad (3)$$

2. Mixing of materials. After weighing, the materials were mixed as intimately as possible by hand with an agate or porcelain mortar and pestle or by using an automatic alumina mortar and pestle. The mixing time varied from about 1 to 1.5 hours.

Preliminary mixing was required if one or more of the three main components were used as basic materials. This was done in 60 gm lots with the ball mill. The mixing time was usually 4 to 5 hours.

D. Sintering

The mixed sample was packed into the platinum-lined alumina crucible with a stainless steel spatula. The covered crucible was covered and put into a pre-heated furnace. After a temperature recovery period of about 10 minutes, the crucible was usually left in the furnace for 2 hours. After this reaction period, it was removed from the furnace and air quenched. The sample was taken from the crucible and ground by hand with a mortar and pestle to prepare it for x-ray diffraction analysis.

E. X-Ray Diffraction Analysis

1. Diffraction patterns. An x-ray diffraction pattern was made of each sintered sample. A 2θ range from 15 to 90° was used on the majority of the samples. These limits were exceeded only in order to check for new peaks that might have appeared as the composition of the sample was varied. A diffractometer speed of 1°/minute and a slit width of 0.1 mm was generally used for the patterns. A slower speed, such as 0.5°/minute, and a narrower slit (0.05 mm), along with other maximizing adjustments on the recorder, were used to increase the resolution of certain peaks. This was important in determining if there was any rhombohedral splitting.

2. Indexing. Each peak on the patterns was accounted for by assigning a value or values of "hkl" or attributing it to a contaminant. Knowing the crystallographic results of the three binary systems helped to provide a basis for

determining the crystallographic structure of a particular sample. The following equations were used to index the patterns:

$$\frac{1}{d^2} = \frac{(h^2+k^2+l^2)\ \sin^2\alpha+2(hk+kl+hl)(\cos^2\alpha-\cos\alpha)}{a^2(1-3\ \cos^2\alpha+2\cos^3\alpha)} \qquad \text{Rhombohedral} \qquad (4)$$

$$\frac{1}{d^2} = \frac{h^2}{a^2} + \frac{k^2}{b^2} + \frac{l^2}{c^2} \qquad \text{Orthorhombic} \qquad (5)$$

$$\frac{1}{d^2} = \frac{h^2+k^2}{a^2} + \frac{l^2}{c^2} \qquad \text{Tetragonal} \qquad (6)$$

A great aid in indexing the rhombohedral patterns was:

$$\cos\alpha = \frac{d_{hkl} - d_{hk\bar{l}}}{2d} \cdot \frac{h^2+k^2+l^2}{(h+k)l} \qquad \text{Rhombohedral Angle} \qquad (7)$$

The values of $\cos^2\alpha$ and $\cos^3\alpha$ were considered to be negligible as $\cos\alpha$ was very small.

The lattice parameters (a,b,c,and α) were determined from the patterns, and the "d" values were calculated for all possible values of "hkl" using a digital computer. The value or values of "hkl" for a certain peak were determined by comparing the "d" value from the pattern with the "d" value of all the possible "hkl" combinations. A pattern was considered to be indexed when all the peaks could be accounted for by using the "hkl" values determined from one of the three crystallographic structure equations.

The volumes of the unit cells were determined using the following equations.

$$V = a^3 \sqrt{1-3\cos^2\alpha + 2\cos^3\alpha} \qquad \text{Rhombohedral} \qquad (8)$$

$$V = abc \qquad \text{Orthorhombic} \qquad (9)$$

$$V = a^2c \qquad \text{Tetragonal} \qquad (10)$$

IV. EXPERIMENTAL RESULTS AND DISCUSSION

A. Sintering

The temperature and time of the sintering process were determined mainly from previous experience with the perovskite type materials. A temperature of 850°C and a time of 2 hours were used for the greater portion of the samples, and the results showed the formation of almost complete solid solutions. The sintering temperature was decreased to 800°C for samples containing 70 and 80 per cent (molar) $BiFeO_3$ and was increased to 900 and 1050°C for samples containing 10 and 0 per cent $BiFeO_3$. The lower sintering temperature was required because Bi_2O_3 has a melting point of 820°C. The sintering temperature varied $\pm$ 8°C during the reaction period due to the type of control.

An alumina (morganite) crucible was used to help prevent loss of Bi_2O_3 by decomposition and evaporation. The high density of this type of crucible made it very suitable to accomplish this objective. The use of the open system did not cause any contamination, nor did it allow more loss of the sample by evaporation than a closed system. It was also found that no detectable amount of contamination was produced by the method utilized to mix the starting materials. This was shown by the x-ray diffraction analyses.

The sintered samples were air quenched in an attempt to obtain single phase products. This was accomplished in all areas of the ternary system except those close to a

phase boundary where mixed perovskite phases were found. According to the x-ray diffraction patterns of the various samples, solid solubility existed in all the regions investigated.

The volume of the sintered sample was usually considerably less than that of the material put into the furnace. In general, the shrinkage and hardness of the sintered sample increased with increasing amounts of $BiFeO_3$. Also, the color of the sintered sample became darker as the $BiFeO_3$ content was increased.

B. Crystallographic Results

1. X-ray diffraction analysis. Powder x-ray diffraction patterns were made of each sintered sample in order to determine its crystallographic structure. A 2θ range from 15 to 90° was usually sufficient to record the necessary pattern. The correct alignment of the diffractometer was found to be an important factor in determining accurate lattice parameters. This factor can best be seen in Table I by considering changes in the trends of the lattice parameters as the sample composition is changed. However, general increases or decreases in a parameter can still be recognized.

The background radiation was greater for some samples than for others. The main reason for this was the sample composition. The background was less for samples in the regions close to 100 percent $PbZrO_3$ or $PbTiO_3$ than for those which had $BiFeO_3$ as their main component. This may

TABLE I

X-RAY DATA OF THE TERNARY SYSTEM

Sample		Parameters				Vol. of One	Phases Present
No.	Composition[a]	a (Å)	b (Å)	c (Å)	α (°)	Unit Cell (Å^3)	
1	100[90:10]-0	4.183			89°50'	71.304	Rhombohedral and ZrO_2
2	95[90:10]-5	4.104			89°52'	69.124	Rhombohedral and ZrO_2
4	90[90:10]-10	5.811	11.615	8.216		69.318	Orthorhombic and ZrO_2
6	80[90:10]-20	5.811	11.659	8.232		69.715	Orthorhombic and ZrO_2
7	70[90:10]-30	5.798	11.615	8.207		69.086	Orthorhombic and ZrO_2
8	60[90:10]-40	5.774	11.518	8.154		67.785	Orthorhombic and ZrO_2
10	50[90:10]-50	5.704	11.315	8.034		64.815	Orthorhombic and ZrO_2
12	40[90:10]-60	5.648	11.242	7.968		63.241	Orthorhombic and ZrO_2
14	30[90:10]-70	5.612	11.167	7.916		62.012	Orthorhombic and ZrO_2
18	80[80:20]-20	4.068			89°57'	67.32]	Rhombohedral and ZrO_2
19	70[80:20]-30	5.750	11.447	8.112		66.741	Orthorhombic and ZrO_2
20	40[80:20]-60	5.648	11.242	7.968		63.241	Orthorhombic and ZrO_2
21	80[75:25]-20	4.064			89°50'	67.121	Rhombohedral and ZrO_2
23	80[70:30]-20	4.068			89°44'	67.321	Rhombohedral and ZrO_2
24	60[70:30]-40	4.038			89°57'	65.840	Rhombohedral and ZrO_2
25	50[70:30]-50	5.676	11.273	8.000		63.986	Orthorhombic and ZrO_2
26	40[70:30]-60	5.656	11.224	7.968		63.229	Orthorhombic and ZrO_2
27	80[60:40]-20	4.038			89°47'	65.840	Rhombohedral and ZrO_2
28	40[60:40]-60	3.980			89°52'	63.043	Rhombohedral and ZrO_2
29	80[50:50]-20	4.000		4.124		65.984	Tetragonal(with Rhombohedral and ZrO_2)
30	70[50:50]-30	4.022		4.006		64.833	Tetragonal and ZrO_2
31	60[50:50]-40	4.017			89°53'	64.818	Rhombohedral and ZrO_2
32	50[50:50]-50	3.996			89°47'	63.808	Rhombohedral and ZrO_2
34	40[50:50]-60	3.984			89°39'	63.234	Rhombohedral

TABLE I (cont.)

Sample		Parameters				Vol. of One	Phases Present
No.	Composition	a (Å)	b (Å)	c (Å)	α (°)	Unit Cell (Å^3)	
35	20[50:50]-80	3.954			89°31'	61.817	Rhombohedral, γ-Bi_2O_3, $Bi_2O_3 \cdot 2Fe_2O_3$
36	90[30:70]-10	3.954		4.127		64.522	Tetragonal and ZrO_2
37	70[30:70]-30	3.934		4.203		65.046	Tetragonal and ZrO_2
38	60[30:70]-40	3.914		4.170		63.880	Tetragonal
39	50[30:70]-50	3.914		4.204		64.404	Tetragonal and ZrO_2
40	40[30:70]-60	3.968			89°39'	62.476	Rhombohedral
41	90[15:85]-10	3.918		4.178		64.136	Tetragonal
42	70[15:85]-30	3.892		4.163		63.061	Tetragonal
44	40[15:85]-60	3.836		4.415		64.967	Tetragonal, γ-Bi_2O_3
45	30[15:85]-70	3.942			89°35'	61.255	Rhombohedral
46	90[10:90]-10	3.882		4.138		62.360	Tetragonal
47	90[5:95]-10	3.890		4.160		62.949	Tetragonal and ZrO_2

[a] The following notation has been used: per cent [$PbZrO_3$:$PbTiO_3$] - per cent $BiFeO_3$.

have been caused by the fluorescence of iron in the $BiFeO_3$. One other possible minor reason was that other x-ray equipment in the same room could have contributed to the background if they were in operation at the same time.

Zirconium oxide was the main and only noticeable non-perovskitic contaminant found in most of the prepared materials. A peak with an average I/I_o value of 7 occured at a "d" value of approximately 3.16 Å, which is the location of the main peak of ZrO_2.

The splitting of peaks on most of the rhombohedral patterns was so small that it was not detectable on the regular 1°/minute scan. Therefore, a slower speed, such as 0.5°/minute, and a narrower slit (0.05 mm) were required to increase the resolution. The peak splitting could then be seen and the rhombohedral angle calculated.

2. Ternary phase diagram. The knowledge of the crystallographic structures of the various samples was used to construct the interior region of the ternary phase diagram (Figure 2). Previous results from the work on the three binary systems were used to determine the phase boundaries on the sides of the ternary diagram. [2,5,11,15] The phase boundaries are indicated with dotted lines because there is a compositional width of the phase transition regions. However, the end points agreed well with the binary systems' phase boundaries. It is not known if distinct phase boundaries exist in this system. The results of the three binary systems have shown two-phase transition

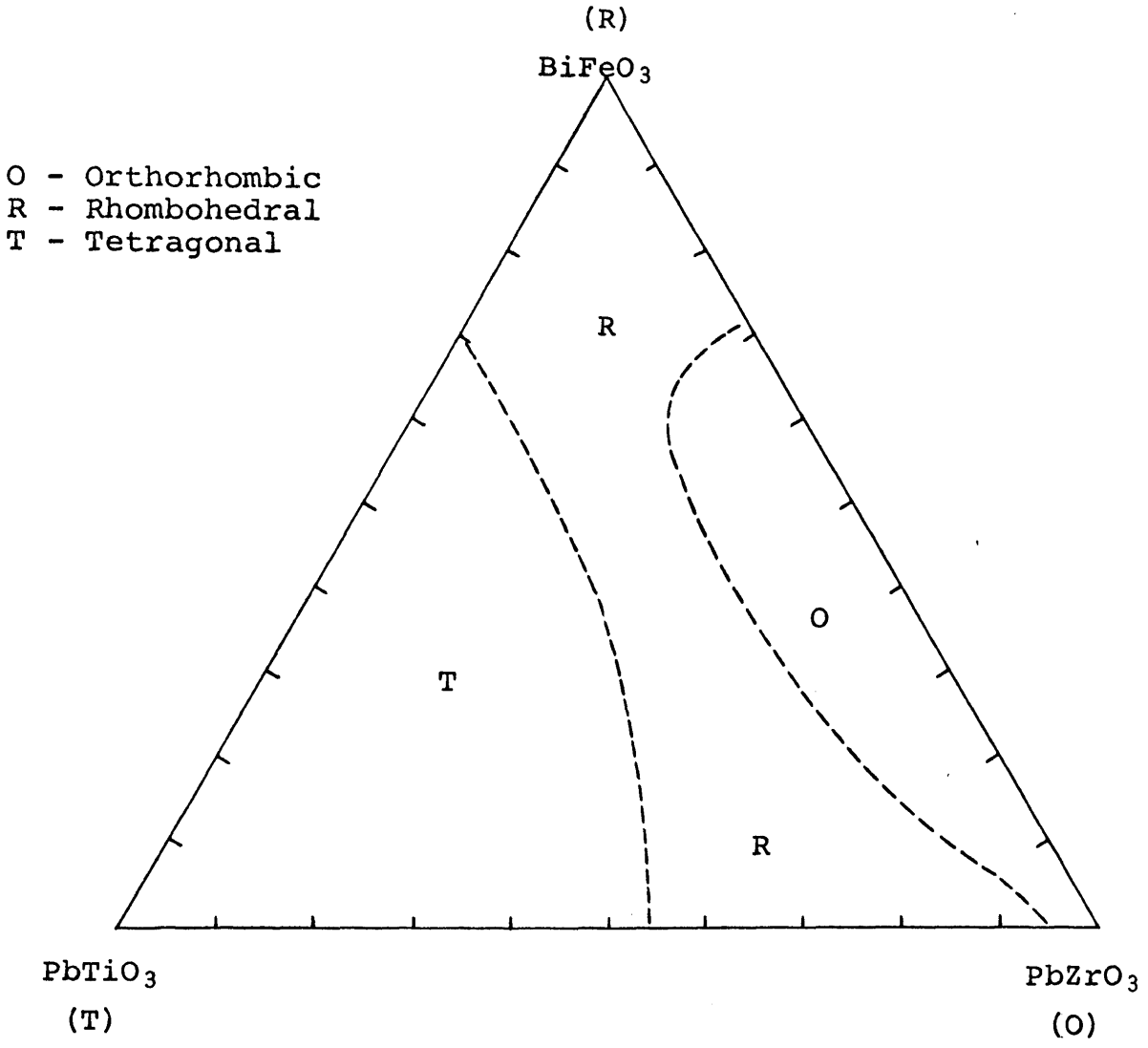

Figure 2. Crystallographic results of this investigation.

regions to exist rather than a distinct phase boundary. The work with this ternary system indicates a two-phase region occurs along each of the phase boundary lines.

The general crystallographic results agree with those of Ikeda and Okano [7] in the region that they investigated (40 to 70 per cent $PbZrO_3$ and up to 50 per cent $BiFeO_3$). However, their values of the lattice parameters ("a" and "c") are slightly larger except for the "c" parameter of the 80 per cent [50 $PbZrO_3$:50 $PbTiO_3$]-20 per cent $BiFeO_3$ sample. The crossing of the tetragonal-rhombohedral phase boundary line on the vertical line (from 50 per cent $PbZrO_3$ to pure $BiFeO_3$) was found to occur between 30 and 40 per cent $BiFeO_3$ in this study. Ikeda and Okano reported it between 30 and 35 per cent $BiFeO_3$ [7] in one article and at 35 per cent $BiFeO_3$ [16] in the earlier short notes of the main article.

The values of the tetragonal c/a ratios (Figure 3) generally agree with expected values in this region. The c/a ratio for the binary $PbTiO_3$-$BiFeO_3$ increases from 1.063 [17] to 1.20 [18] for 0 to 70 per cent $BiFeO_3$, respectively. The addition of $PbZrO_3$ to the binary suppresses this increasing ratio until 50 $PbZrO_3$:50 $PbTiO_3$ is reached; here, additions of $BiFeO_3$ decreases the ratio.

The orthorhombic region of the system was indexed using a multiple-cell orthorhombic structure. The previous work by Chou [15] indicated that this region could be indexed with this structure. It is possible that a ferroelectric

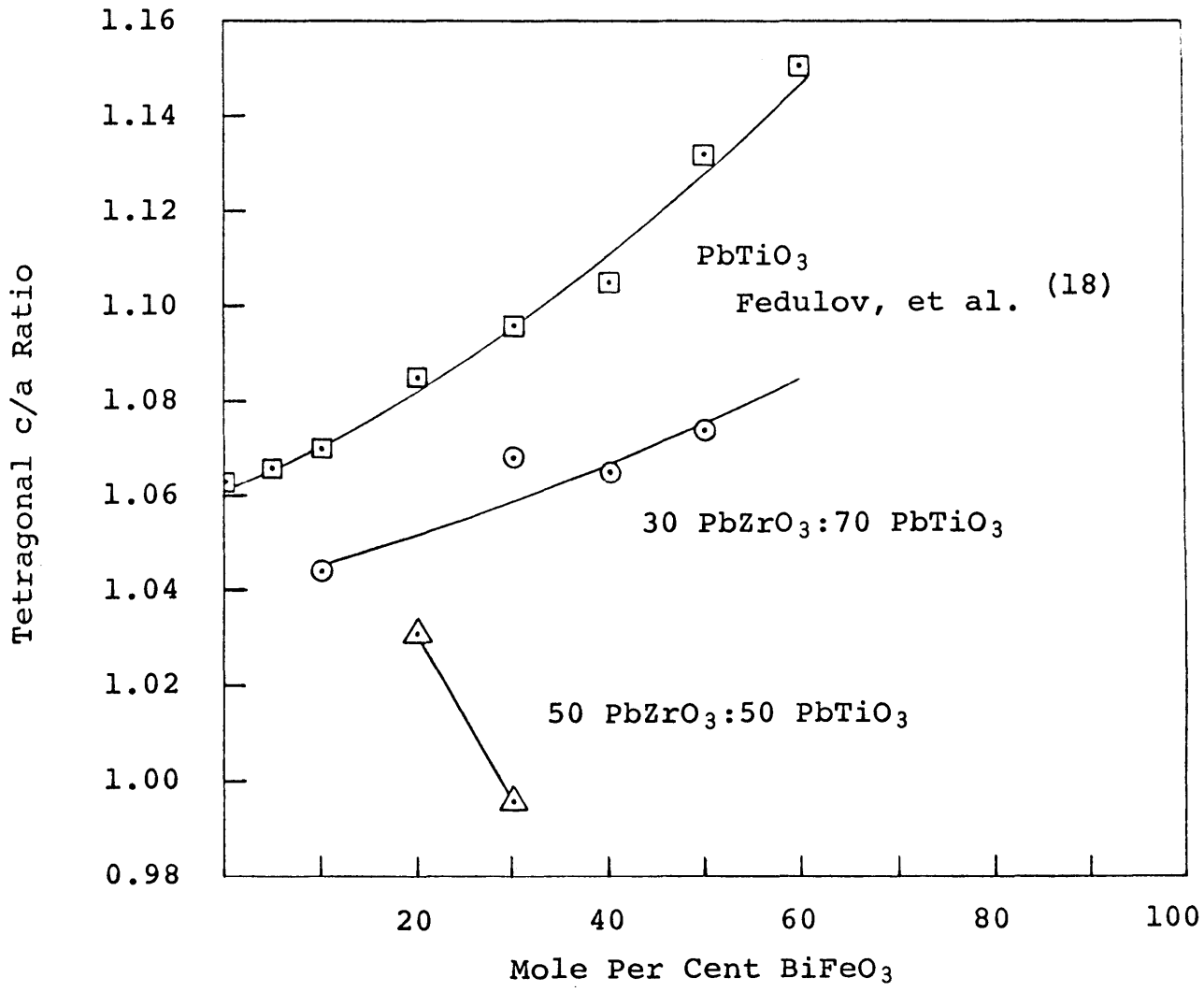

Figure 3. Variation of tetragonal c/a ratio for different amounts of $BiFeO_3$.

orthorhombic region exist in the ternary system as in the $PbZrO_3$-$BiFeO_3$ binary system; however, conclusive electrical measurements have not been made at this time.

Generally, all three lattice parameters decreased with additions of $BiFeO_3$ (Figure 4). However, the calculated volume of the unit cell did not consistently decrease, although there was an overall decrease. This decrease is shown in Table I. The volumes of unit cell showing consistent decreases are presented in Figure 5.

The rhombohedral angle was less near the tetragonal than the orthorhombic region. The distortion increased and the "a" parameter decreased with additions of $BiFeO_3$ as shown in Figure 6 for 50 $PbZrO_3$:50 $PbTiO_3$.

C. Electrical Properties*

The dielectric constant and Curie point were determined for various ratios of $BiFeO_3$ and 50 $PbZrO_3$:50 $PbTiO_3$. The Curie point was found to be 380 and 400°C for 20 and 30 per cent $BiFeO_3$, respectively. These values are 25°C higher than the ones reported by Ikeda and Okano, [7] which would indicate greater perfection of the materials used in this study. The measured dielectric constants (Figure 7) were much higher than those reported by Ikeda and

---

* Electrical measurements were performed in the Department of Physics by co-workers.

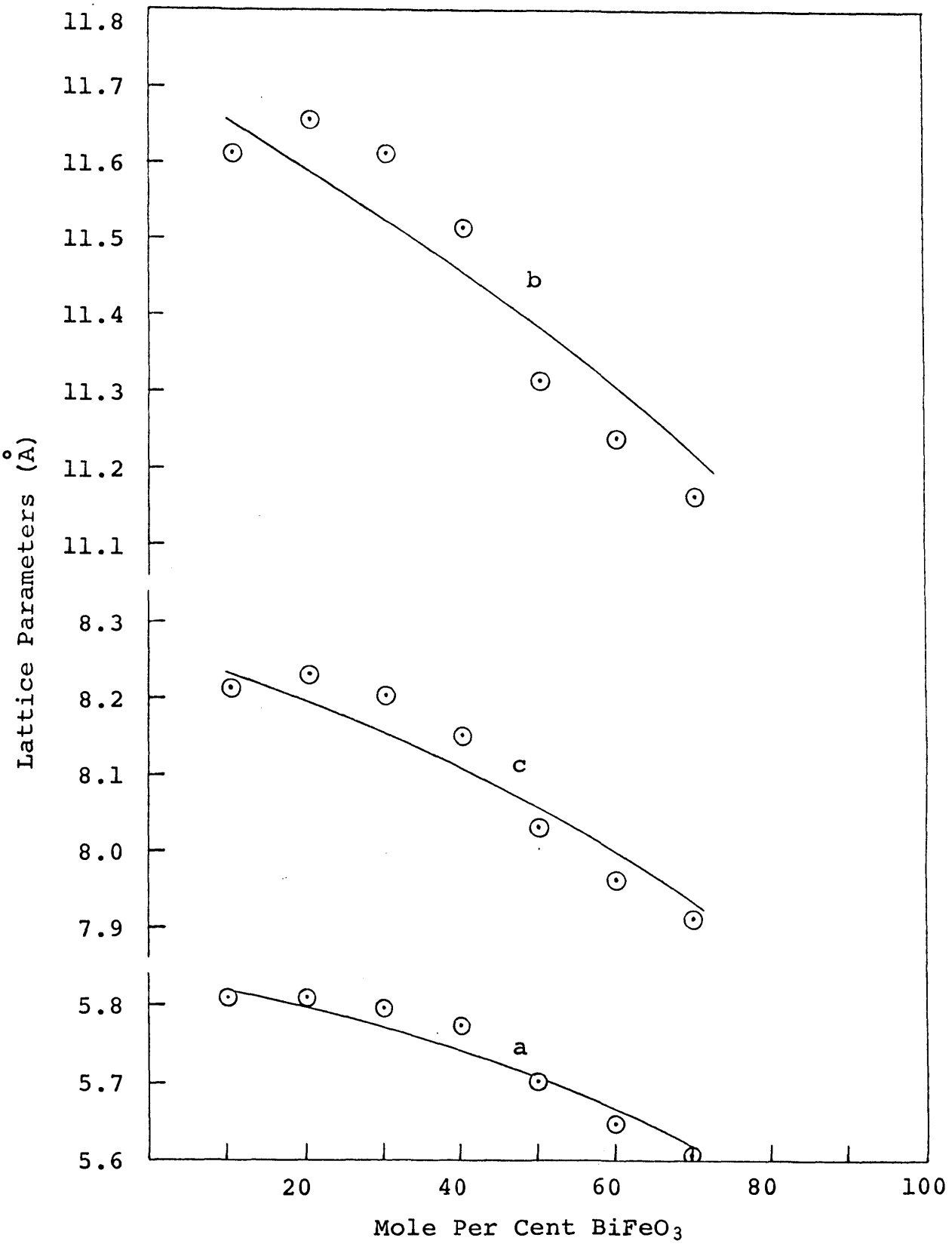

Figure 4. Lattice Parameters of 90 $PbZrO_3$:10 $PbTiO_3$ with varying amounts of $BiFeO_3$.

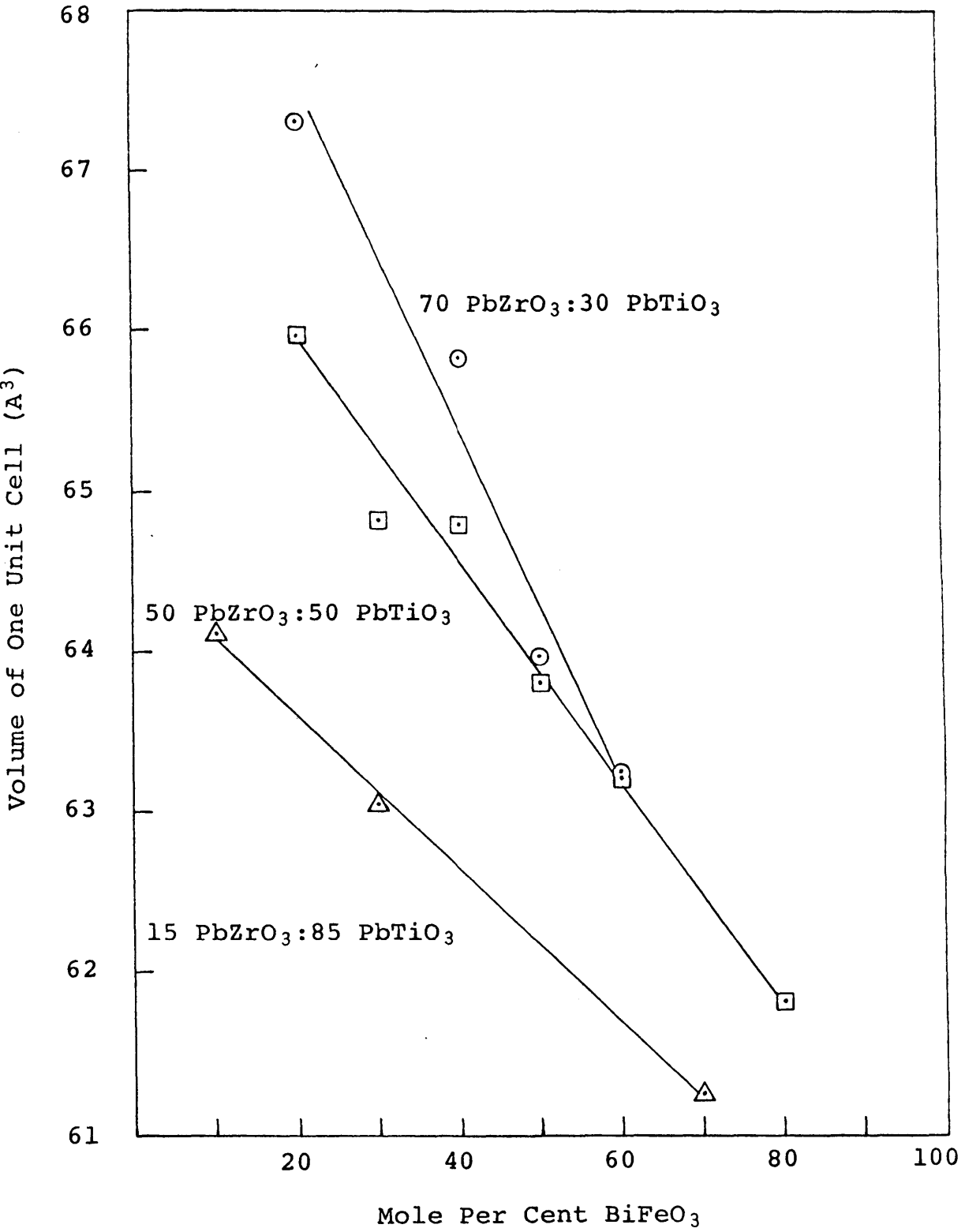

Figure 5. Variation of the volume of one unit cell for different amounts of $BiFeO_3$.

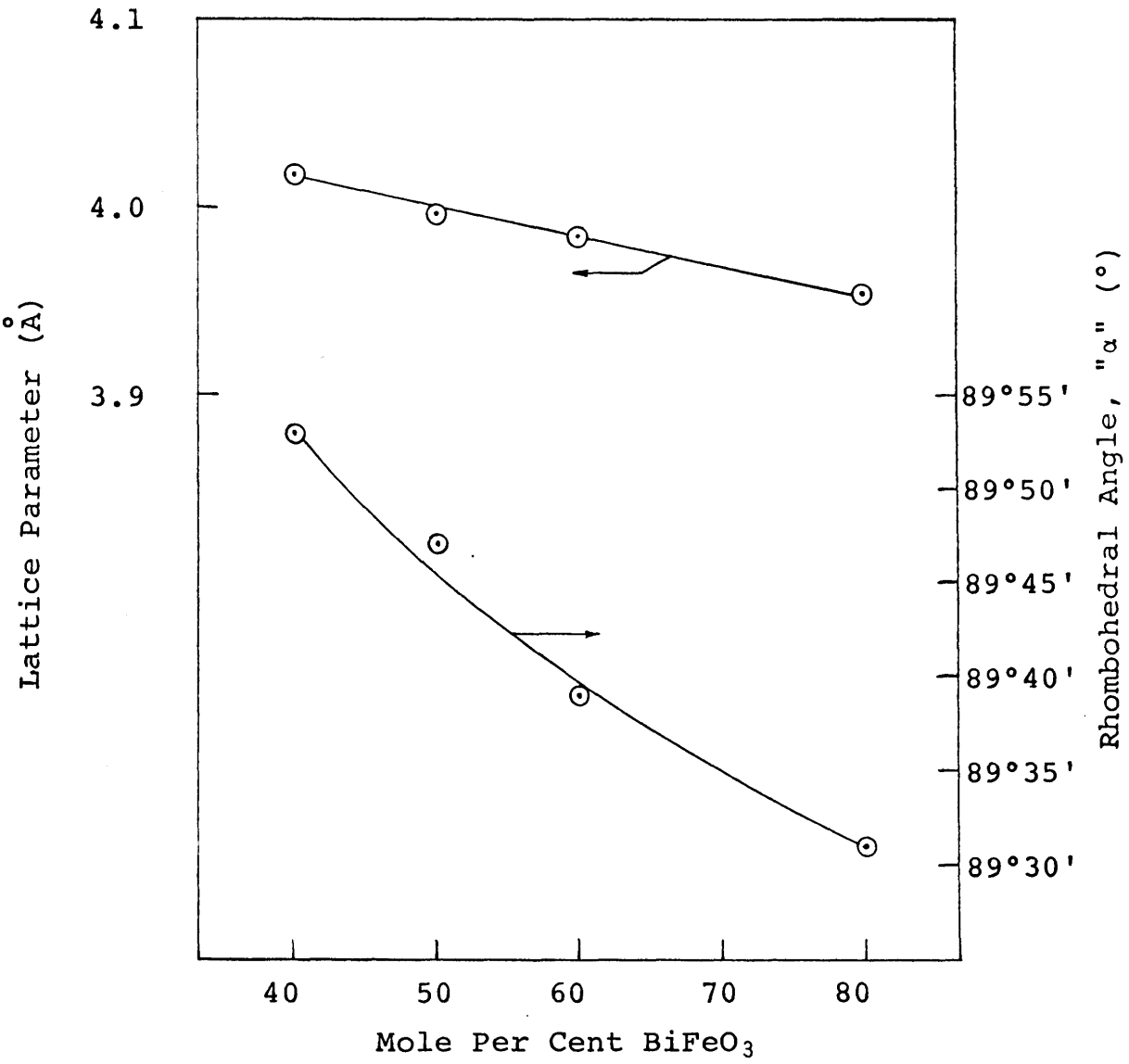

Figure 6. Rhombohedral lattice parameters of 50 $PbZrO_3$:50 $PbTiO_3$ and varying amounts of $BiFeO_3$.

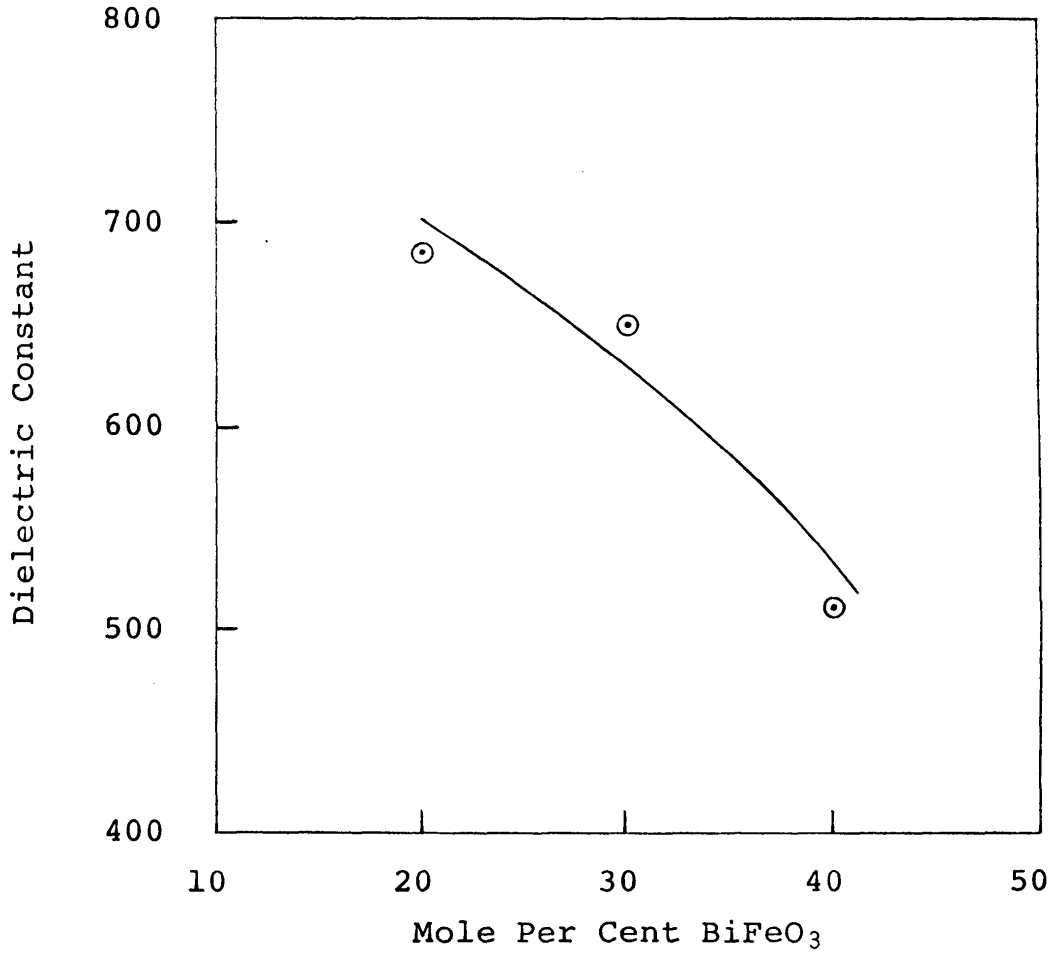

Figure 7. Dielectric constant of 50 $PbZrO_3$: 50 $PbTiO_3$ and different amounts of $BiFeO_3$ at room temperature using Fire-On silver electrodes.

Okano. [7] For 20 per cent $BiFeO_3$, they reported 500 compared to 685 found in this study. The present study finds significantly higher electrical properties than those reported previously. The less dense ceramics used in the prior study might explain the difference.

BIBLIOGRAPHY

1. Gerson, R., P. Chou, and W. James (1966) Ferroelectric Properties in $PbZrO_3$-$BiFeO_3$ Solid Solutions. Submitted to Journal of Applied Physics.

2. Fedulov, S., P. Ladyzhinskii, I. Pyatigorskaya, and Y. Venevtsev, Soviet Physics - Solid State, 6, 375 (1964).

3. Shirane, G. and A. Takeda, J. Phys. Soc. Japan, 7, 5 (1952).

4. Shirane, G., K. Suzuki, and A. Takeda, J. Phys. Soc. Japan, 7, 12 (1952).

5. Sawaguchi, E., J. Phys. Soc. Japan, 8, 615 (1953).

6. Jaffe, B., R. Roth, and S. Marzulla, J. Appl. Phys., 25, 809 (1954).

7. Ikeda, T. and T. Okano, Jap. J. Appl. Phys., 3, 63 (1964).

8. Kiselev, S., R. Ozerov, and G. Zhdanov, Soviet Physics-Doklady, 7, 742 (1962).

9. Roginskaya, Y., Y. Venevtsev, S. Fedulov, and G. Zhdanov, Soviet Physics - Cryst., 8, 490 (1963).

10. Smolenskii, G., V. Yudin, E. Sher, and U. Stolypin, Soviet Physics - JETP, 16, 622 (1962).

11. Gerson, R and W. James (1966) Ferroelectric Properties of $BiFeO_3$ and Related Materials, Progress Report to U. S. Atomic Energy Commission, AEC AT(11-1)-1368.

12. Venevtsev, Y. et al., Iav. Akad. Nauk. SSSR, Ser. Fiz., 28, 683 (1964).

13. Berlincourt, D. and H. Krueger (1963) Annual Progress Report to Sandia Corporation, Purchase Order 51-6529.

14. Ivanova, V., U. Tomeishvili, S. Fedulov, and Y. Venevtsev, Vopr. Radioelektroniki Ser. 3, Detali i Komponenty Apparatury, 10, 86 (1962).

15. Chou, P. (1966) Masters thesis, Library, University of Missouri at Rolla (1966).

16. Ikeda, T. and T. Okano, Jap. J. Appl. Phys., 2, 63 (1963).

17. Megaiv, H., Proc. Phys. Soc. (London), 58, 10 (1946).

18. Fedulov, S., G. Venevtsev, G. Zhdanov, E. Smazhevskaya, and I. Rez. Soviet Physics - Cryst., 7, 62 (1962).

19. Sawaguchi, E., Structure Reports, 16, 254 (1952).

20. Filip'ev, V., N. Smalyaninov, E. Fesenko, and I Belyaev, Soviet Physics - Cryst., 5, 913 (1960).

APPENDICES

A. MATERIALS

B. APPARATUS

C. SINTERING DATA

D. X-RAY DIFFRACTION DATA FOR $PbZrO_3$, $PbTiO_3$, AND $BiFeO_3$

E. X-RAY DIFFRACTION DATA FOR THE TERNARY SYSTEM

APPENDIX A

MATERIALS

The following is a list of the materials used in this investigation. A detailed analysis of each may be obtained from the chemical catalog of the respective manufacturer.

1. Lead oxide (PbO). Laboratory chemical grade (mono-yellow), Fisher Scientific Company, Fairlawn, N. J.

2. Zirconium oxide (ZrO_2). Laboratory chemical grade, Fisher Scientific Company, Fairlawn, N. J.

3. Titanium oxide (TiO_2). Certified reagent grade, Fisher Scientific Company, Fairlawn, N. J.

4. Bismuth trioxide (Bi_2O_3). Certified reagent grade, Fisher Scientific Company, Fairlawn, N. J.

5. Iron oxide (Fe_2O_3). Chemically pure grade, J. T. Baker Chemical Company, Phillipsburg, N. J.

APPENDIX B

APPARATUS

The following is a list of the main apparatus used in this investigation:

1. Analytical Balance. Sartorius (multi-purpose), Type 2403 (single-pan), 0-100 gm, Aloe Scientific Company, St. Louis, Missouri.

2. Analytical Balance. Chicago Apparatus Company, Model 340-D (two-pan), Voland and Sons, Inc., New Rochell, N. Y.

3. Mortar and Pestle. Agate, Fisher Scientific Company, Fairlawn, N. J.

4. Mortar and Pestle. Porcelain, Fisher Scientific Company, Fairlawn, N. J.

5. Mortar and Pestle. Alumina (automatic), Model 155, Fisher Scientific Company, Fairlawn, N. J.

6. Ball Mill. Variable speed, located in Graduate Center for Materials Research, University of Missouri at Rolla.

7. Crucible. Recrystallized alumina, Type N4429, Morgan Refractories, England.

8. Platinum Foil. High purity, 0.001 inch thickness, A. D. Mackey, Inc., New York, N. Y.

9. Furnace. Electrical, platinum-wound resistance, located in Chemical Engineering building, University of Missouri at Rolla.

10. Furnace. Electrical, Kanthal-wound resistance, located in Graduate Center for Materials Research, University of Missouri at Rolla.

11. Diffractometer. General Electric, Model BR, Type 1, General Electric Company, Kansas City, Missouri.

12. Diffractometer. Siemens Crystalloflex IV, Type U 13, Siemens America, Inc., Long Island, N. Y.

APPENDIX C

TABLE II

SINTERING DATA

Sample		Time		Temp.	Preparation		
No.	Composition[a]				Time	Method[b]	Constituents[c]
		hrs.		°C	hrs.		
1	100[90:10]-0	2		1050	1.50	Hand	MO
2	95[90:10]-5	2		900	0.50	Hand	BM
3	90[90:10]-10	2		900	1.50	Hand	MO
4	90[90:10]-10	2	1/3	900	1.50	Hand	BM
5	80[90:10]-20	2		850	1.50	Hand	MO
6	80[90:10]-20	2		850	4.00	Ball Mill	BM
7	70[90:10]-30	2		850	1.50	Hand	MO
8	60[90:10]-40	2		880	1.50	Hand	MO
9	50[90:10]-50	2		850	1.25	Hand	BM
10	50[90:10]-50	2		850	1.25	Hand	BM
11	40[90:10]-60	2		850	1.25	Hand	BM
12	40[90:10]-60	1	5/6	850	1.25	Hand	BM
13	30[90:10]-70	2		850	1.00	Hand	BM
14	30[90:10]-70	2		850	1.00	Hand	BM
15	100[80:20]-0	2		1050	1.50	Hand	MO
16	100[80:20]-0[d]	2		1050	1.50	Hand	MO
17	100[80:20]-0[e]	2		1050	1.50	Hand	MO
18	80[80:20]-20	2	3/4	850	1.00	Auto	BM
19	70[80:20]-30	2		850	1.25	Auto	BM
20	40[80:20]-60	2	1/6	850	1.25	Auto	BM
21	80[75:25]-20	2		850	1.25	Auto	BM
22	80[70:30]-20	2		850	1.50	Auto	BM
23	80[70:30]-20	2		850	1.50	Auto	BM
24	60[70:30]-40	2		850	1.50	Auto	BM
25	50[70:30]-50	2		850	1.50	Auto	BM
26	40[70:30]-60	2	3/4	850	1.50	Auto	BM
27	80[60:40]-20	2		850	2.00	Auto	BM
28	40[60:40]-60	2		850	0.50	Hand	BM
29	80[50:50]-20	2		850	1.25	Auto	BM
30	70[50:50]-30	2		850	1.50	Auto	BM
31	60[50:50]-40	2		850	1.50	Hand	BM
32	50[50:50]-50	1	5/6	850	1.50	Auto	BM
33	40[50:50]-60	2		850	1.25	Auto	BM
34	40[50:50]-60	2	1/6	800	1.25	Auto	BM
35	20[50:50]-80	2	1/6	800	2.00	Auto	BM
36	90[30:70]-10	2		850	1.50	Auto	BM
37	70[30:70]-30	2		850	1.50	Auto	BM

TABLE II (cont.)

Sample		Time	Temp.	Preparation		
No.	Composition[a]			Time	Method[b]	Constituents[c]
		hrs.	°C	hrs.		
38	60[30:70]-40	4[f]	850	1.00	Auto	BM
39	50[30:70]-50	2	850	1.50	Auto	BM
40	40[30:70]-60	2	850	1.00	Auto	BM
41	90[15:85]-10	2 1/6	900	1.50	Auto	BM
42	70[15:85]-30	4[f]	850	1.75	Auto	BM
43	40[15:85]-60	2	850	2.00	Auto	BM
44	40[15:85]-60	2	850	1.50	Auto	BM
45	30[15:85]-70	2	850	2.00	Auto	BM
46	90[10:90]-10	2	890	1.50	Auto	BM
47	90[5:95]-10	2	850	2.00	Auto	BM

[a] The following notation has been used: per cent [$PbZrO_3$: $PbTiO_3$] - per cent $BiFeO_3$.
[b] Samples were prepared by hand mixing and grinding with mortar and pestle or by using automatic mortar and pestle.
[c] Ball milling (BM) was used in preparing the ternary components of the samples, except for the ones marked "MO" in which the mixed oxides were used as consituents.
[d] Pressed with 19,500 psi and extra $PbZrO_3$ added.
[e] Pressed with 19,500 psi, extra $PbZrO_3$ added, and 0.8 per cent weight loss.
[f] Put back in furnace for an additional 2 hour period because volume shrinkage was much less than normal.

APPENDIX D

X-RAY DIFFRACTION DATA FOR $PbZrO_3$, $PbTiO_3$, AND $BiFeO_3$

A. Calculated Values of "d" and "hkl" for the Orthorhombic Multiple Cell of $PbZrO_3$[a]

Parameters: a = 5.872 Å, b = 11.744 Å, c = 8.202 Å

d (Å)	hkl
5.2521	110
4.1521	120
4.1010	002
3.2572	130
3.2323	112
3.0272	131
2.9360	200,040
2.8483	210
2.7642	041,201
2.5506	132
2.3873	042,202
2.3488	050,230
2.0761	240
2.0505	004
1.9307	310
1.8569	320
1.8385	124
1.7507	330
1.6916	322
1.6811	204,044
1.6641	214
1.6101	332
1.5037	350
1.4680	400
1.4651	135
1.4589	244
1.4118	352
1.3726	412
1.3314	026
1.3130	440
1.3033	432
1.2449	450
1.1970	335
1.1815	236
1.1417	434
1.1249	530
1.1144	531
1.1037	522

A. (cont.)

d (Å)	hkl
1.1057	444
1.1009	326

[a] Reported by Sawaguchi [19] at 20°C for CuKα radiation.

B. X-ray Data for Rhombohedral Distorted Perovskite Lattice of $BiFeO_3$[b]

Parameters: a = 3.957 Å, α = 89°28'

d (Å)	I/I_o	hkl
3.96	4	100
2.82	10	110
2.79	10	$1\bar{1}0$
2.31	1	111
		$\bar{1}11$
2.28	3	$1\bar{1}1$
		$11\bar{1}$
1.98	4	200
1.78	5	210
1.76	5	$2\bar{1}0$
1.62	3	211
		$\bar{2}11$
1.61	8	$2\bar{1}1$
		$21\bar{1}$
1.406	2	220
1.392	2	$2\bar{2}0$
1.329	4	$22\bar{1}$
1.317	4	300
		$\bar{2}21$
1.312	4	$2\bar{2}1$
1.253	4	310
1.245	4	$3\bar{1}0$
1.214	1	311
1.200	2	$3\bar{1}1$
		$31\bar{1}$
1.192	2	$\bar{3}11$
1.155	1	222

B. (cont.)

d (Å)	I/I_o	hkl
		$\bar{2}22$
1.138	3	$2\bar{2}2$
		$22\bar{2}$
1.103	5	$32\bar{0}$
1.092	4	$3\bar{2}0$
1.066	4	$32\bar{1}$
1.060	4	$3\bar{2}\bar{1}$
1.053	7	$\bar{3}21$
		$3\bar{2}1$
0.989	2	400

[b] Reported by Filip'ev, et al. [20] for FeKα radiation.

C. X-ray Data for Tetragonal $PbTiO_3$ [c]

Parameters: a = 3.905 Å, c = 4.151 Å

d (Å)	I/I_o	hkl
4.150	26	001
3.899	49	100
2.842	100	101
2.758	52	110
2.297	40	111
2.076	15	002
1.950	32	200
1.833	13	102
1.765	10	201
1.744	11	210
1.658	19	112
1.608	42	211
1.421	13	202
1.384	3	003
1.379	9	220
1.335	7	212
1.308	3	221
1.3045	5	103
1.3000	11	300
1.2403	10	301
1.237	3	113

C. (cont.)

d (Å)	I/I_o	hkl
1.2333	7	310
1.1819	10	311
1.1484	5	222
1.1287	3	203
1.1016	2	302
1.0841	7	213
1.0816	3	320
1.0601	9	312
1.0465	8	321
1.0383	1	004
1.0031	2	104
0.9766	3	223
0.9747	4	400
0.9715	1	114
0.9593	3	322
0.9491	2	401
0.9476	2	303
0.9457	4	410
0.9222	6	411

[c] Taken from ASTM card number 6-0452.

APPENDIX E

X-RAY DIFFRACTION DATA FOR THE TERNARY SYSTEM

Notes:

1. All x-ray patterns are based on Cu Kα radiation with a wavelength of 1.542 Å.
2. For the orthorhombic patterns, the "a", "b", and "c" parameters were calculated from the "400", "240", and "004" lines, respectively, using equation 5.
3. In the rhombohedral region, the angle was determined by using either equation 4 or 7. The line or pair of lines used for this calculation are indicated after each "α" value in the following tables. The "a" parameter was calculated using the "200" line.
4. The "a" and "c" tetragonal parameters were determined using the "200" and "211" lines, respectively, and equation 6.
5. The following notation has been used in designating the composition of the various samples: per cent [$PbZrO_3$:$PbTiO_3$]-per cent $BiFeO_3$.

A. Composition: 100[90:10]-0

Structure: Rhombohedral
Parameters: a = 4.183 Å, α = 89°50' (110 and $1\bar{1}0$)

2θ (°)	d (Å)	I/I_o	hkl
21.30	4.183	17	100
27.30	3.264	1	(ZrO_2)
30.42	2.954	100	$1\bar{1}0$
			$11\bar{1}$
37.50	2.413	13	$1\bar{1}1$
			$\bar{1}11$
43.60	2.091	34	200
49.00	1.872	12	210
54.25	1.707	37	$2\bar{1}1$
			$21\bar{1}$
63.50	1.477	11	$2\bar{2}0$
67.70	1.394	3	$22\bar{1}$,300
72.10	1.324	11	310
76.20	1.261	2	$3\bar{1}1$
			$31\bar{1}$
			$\bar{2}22$
80.30	1.207	3	$2\bar{2}2$
			$22\bar{2}$
83.90	1.161	2	320
88.30	1.118	8	$32\bar{1}$

B. Composition: 95[90:10]-5

Structure: Rhombohedral
Parameters: a = 4.104 Å, α = 89°52' (211 and $21\bar{1}$)

2θ (°)	d (Å)	I/I_o	hkl
21.80	4.104	17	100
27.90	3.195	3	(ZrO_2)
30.95	2.899	100	$1\bar{1}0$
37.90	2.373	5	111
			$\bar{1}11$
38.10	2.368	11	$1\bar{1}1$
			$11\bar{1}$
44.10	2.052	28	200
49.55	1.837	7	210
54.60	1.678	13	211
54.75	1.675	25	$2\bar{1}1$
			$21\bar{1}$
63.85	1.452	5	220

B. (cont.)

2θ (°)	d (Å)	I/I_o	hkl
64.10	1.450	7	$2\bar{2}0$
68.25	1.368	4	$22\bar{1}$,300
72.65	1.298	8	$31\bar{0}$
88.90	1.097	6	$32\bar{1}$

C. Composition: 90[90:10]-10

Structure: Orthorhombic
Parameters: a = 5.811 Å, b = 11.615 Å, c = 8.216 Å

2θ (°)	d (Å)	I/I_o	hkl
21.75	4.108	20	002,120
27.85	3.200	4	(ZrO_2)
30.85	2.905	100	200,040,122
38.00	2.372	9	042,202
44.05	2.054	24	004,240
49.50	1.837	5	320,124,242
54.70	1.677	23	322,204,044
64.05	1.453	7	400
72.70	1.299	7	440
89.00	1.098	3	444

D. Composition: 80[90:10]-20

Structure: Orthorhombic
Parameters: a = 5.811 Å, b = 11.659 Å, c = 8.232 Å

2θ (°)	d (Å)	I/I_o	hkl
21.50	4.116	10	002,120
27.60	3.229	2	(ZrO_2)
30.65	2.906	100	200,040,122
37.80	2.376	11	042,202
43.95	2.050	23	004,240
49.60	1.840	2	320,124,242
54.65	1.679	24	322,204,044
64.05	1.453	7	400

D. (cont.)

2 (°)	d (Å)	I/I_o	hkl
72.70	1.300	5	440
81.10	1.187	1	404
89.10	1.099	4	444

E. Composition: 70[90:10]-30

Structure: Orthorhombic
Parameters: a = 5.798 Å, b = 11.615 Å, c = 8.207 Å

2 (°)	d (Å)	I/I_o	hkl
21.60	4.103	16	002,120
28.00	3.184	3	(ZrO)
30.80	2.902	100	200,040,122
37.90	2.369	12	042,202
44.10	2.052	23	004,240
49.70	1.835	2	320,124,242
54.80	1.675	24	322,204,044
64.20	1.449	8	400
73.00	1.297	5	440
81.40	1.184	1	404
89.50	1.096	3	444

F. Composition: 60[90:10]-40

Structure: Orthorhombic
Parameters: a = 5.774 Å, b = 11.518 Å, c = 8.154 Å

2 (°)	d (Å)	I/I_o	hkl
21.70	4.077	15	002,120
28.00	3.184	5	(ZrO)
31.00	2.887	100	200,040,122
38.10	2.354	12	042,202
44.40	2.039	24	004,240
49.90	1.824	2	320,124,242
55.00	1.665	26	322,204,044
64.50	1.443	8	400
73.20	1.290	5	440
81.60	1.178	2	404
89.80	1.090	3	444

G. Composition: 50[90:10]-50

Structure: Orthorhombic
Parameters: a = 5.704 Å, b = 11.315 Å, c = 8.034 Å

2θ (°)	d (Å)	I/I_o	hkl
22.30	4.017	16	002,120
28.60	3.118	8	(ZrO_2)
31.60	2.835	100	200,040,122
38.80	2.319	11	042,202
45.10	2.008	19	004,240
50.75	1.797	1	320,124,242
55.90	1.642	20	322,204,044
65.40	1.426	6	400
74.30	1.273	3	440

H. Composition: 40[90:10]-60

Structure: Orthorhombic
Parameters: a = 5.648 Å, b = 11.242 Å, c = 7.968 Å

2θ (°)	d (Å)	I/I_o	hkl
22.50	3.984	22	002,120
28.60	3.118	11	(ZrO_2)
31.80	2.824	100	200,040,122
39.20	2.297	15	042,202
45.50	1.992	19	004,240
51.10	1.785	4	320,124,242
56.40	1.629	19	322,204,044
66.10	1.412	6	400
75.00	1.262	4	440

I. Composition: 30[90:10]-70

Structure: Orthorhombic
Parameters: a = 5.612 Å, b = 11.167 Å, c = 7.916 Å

2θ (°)	d (A)	I/I_o	hkl
22.60	3.950	24	002,120
28.30	3.151	13	(ZrO_2)

I. (cont.)

2θ (°)	d (Å)	I/I_o	hkl
32.05	2.806	100	200,040,122
39.40	2.285	16	042,202
45.80	1.979	19	004,240
56.80	1.619	21	322,204,044
66.60	1.403	6	400
75.50	1.254	3	440

J. Composition: 80[80:20]-20

Structure: Rhombohedral

Parameters: a = 4.068 Å, α = 89°57' $(11\bar{1})$

2θ (°)	d (Å)	I/I_o	hkl
21.90	4.068	18	100
28.00	3.184	4	(ZrO_2)
31.10	2.876	100	$1\bar{1}0$
			$\bar{1}11$
38.30	2.348	13	$1\bar{1}1$
			$11\bar{1}$
44.50	2.034	23	200
50.00	1.819	5	210
55.25	1.661	22	$2\bar{1}1$
			$21\bar{1}$
64.65	1.438	7	$2\bar{2}0$
73.35	1.286	6	$31\bar{0}$
89.80	1.087	3	$32\bar{1}$

K. Composition: 70[80:20]-30

Structure: Orthorhombic

Parameters: a = 5.750 Å, b = 11.447 Å, c = 8.112 Å

2θ (°)	d (Å)	I/I_o	hkl
22.05	4.056	13	002,120
28.30	3.151	4	(ZrO_2)
31.25	2.875	100	200,040,122
38.50	2.336	13	042,202
44.65	2.028	21	004,240

K. (cont.)

2θ (°)	d (Å)	I/I_o	hkl
50.25	1.814	3	320,124,242
55.35	1.658	23	322,204,044
64.80	1.437	8	400
74.70	1.270	6	440

L. Composition: 40[80:20]-60

Structure: Orthorhombic

Parameters: a = 5.648 Å, b = 11.242 Å, c = 7.968 Å

2θ (°)	d (Å)	I/I_o	hkl
22.50	3.984	22	002,120
28.60	3.118	13	(ZrO_2)
31.80	2.824	100	200,040,122
39.20	2.296	13	042,202
45.50	1.992	18	004,240
51.25	1.785	2	320,124,242
56.40	1.629	20	322,204,044
66.10	1.412	7	400
75.00	1.262	3	440

M. Composition: 80[75:25]-20

Structure: Rhombohedral

Parameters: a = 4.064 Å, α = 98°50' (111 and $11\bar{1}$)

2θ (°)	d (Å)	I/I_o	hkl
22.00	4.064	16	100
28.20	3.162	4	(ZrO_2)
31.20	2.870	100	$1\bar{1}0$
			$\bar{1}11$
38.40	2.345	12	$1\bar{1}1$
			$11\bar{1}$
44.55	2.032	22	200
50.20	1.819	5	210
55.30	1.658	21	$2\bar{1}1$
			$21\bar{1}$
64.80	1.435	5	$2\bar{2}0$

M. (cont.)

2θ (°)	d (Å)	I/I_o	hkl
73.45	1.286	3	310
90.00	1.086	2	$32\bar{1}$

N. Composition: 80[70:30]-20

Structure: Rhombohedral

Parameters: a = 4.068 Å, α = 89°44' ($11\bar{1}$)

2θ (°)	d (Å)	I/I_o	hkl
21.90	4.068	20	100
28.10	3.173	3	(ZrO_2)
31.10	2.871	100	$1\bar{1}0$ $\bar{1}11$
38.35	2.345	13	$1\bar{1}1$ $11\bar{1}$
44.50	2.034	21	200
50.15	1.822	5	210
55.30	1.660	20	$2\bar{1}1$ $21\bar{1}$
64.80	1.435	6	$2\bar{2}0$
73.50	1.288	6	310
90.20	1.088	4	$32\bar{1}$

O. Composition: 60[70:30]-40

Structure: Rhombohedral

Parameters: a = 4.038 Å, α = 89°57' ($11\bar{1}$)

2θ (°)	d (Å)	I/I_o	hkl
22.00	4.038	20	100
28.25	3.156	4	(ZrO_2)
31.30	2.855	100	$1\bar{1}0$ $\bar{1}11$
38.60	2.331	14	$1\bar{1}1$ $11\bar{1}$
44.85	2.019	17	200
50.60	1.806	3	210
55.65	1.648	17	$2\bar{1}1$ $21\bar{1}$

O. (cont.)

2θ (°)	d (Å)	I/I_o	hkl
65.25	1.427	5	$2\bar{2}0$
74.10	1.277	3	310

P. Composition: 50[70:30]-50

Structure: Orthorhombic

Parameters: a = 5.676 Å, b = 11.273 Å, c = 8.000 Å

2θ (°)	d (Å)	I/I_o	hkl
22.40	4.000	20	002,120
28.60	3.118	12	(ZrO_2)
31.70	2.838	100	200,040,122
39.00	2.304	13	042,202
45.30	2.000	18	004,240
56.15	1.637	16	322,204,044
65.75	1.419	5	400
74.65	1.267	3	440

Q. Composition: 40[70:30]-60

Structure: Orthorhombic

Parameters: a = 5.656 Å, b = 11.224 Å, c = 7.968 Å

2θ (°)	d (Å)	I/I_o	hkl
22.45	3.984	21	002,120
28.55	3.124	9	(ZrO_2)
31.85	2.828	100	200,040,122
39.20	2.294	15	042,202
45.50	1.992	17	004,240
51.24	1.787	3	320,124,242
56.45	1.631	17	322,204,044
66.00	1.414	7	400
75.10	1.263	3	440

R. Composition: 80[60:40]-20

Structure: Rhombohedral

Parameters: $a = 4.038$ Å, $\alpha = 89°47'$ (111 and $11\bar{1}$)

2θ (°)	d (Å)	I/I_o	hkl
22.10	4.038	21	100
28.30	3.151	5	(ZrO_2)
31.40	2.851	100	$1\bar{1}0$
38.45	2.339	8	111 $\bar{1}11$
38.65	2.329	15	$1\bar{1}1$ $11\bar{1}$
44.85	2.019	24	200
50.40	1.808	8	$2\bar{1}0$
55.70	1.648	21	$2\bar{1}1$ $21\bar{1}$
65.20	1.425	8	$2\bar{2}0$
74.00	1.278	6	310

S. Composition: 40[60:40]-60

Structure: Rhombohedral

Parameters: $a = 3.980$ Å, $\alpha = 89°52'$ ($11\bar{1}$)

2θ (°)	d (Å)	I/I_o	hkl
22.45	3.980	27	100
28.45	3.135	8	(ZrO_2)
31.80	2.812	100	$1\bar{1}0$ $\bar{1}11$
39.20	2.296	17	$1\bar{1}1$ $11\bar{1}$
45.55	1.990	14	200
51.10	1.781	3	$2\bar{1}0$
56.45	1.624	14	$2\bar{1}1$ $21\bar{1}$
66.20	1.406	5	$2\bar{2}0$
75.25	1.259	4	310

T. Composition: 80[50:50]-20

Structure: Tetragonal (mainly)
Parameters: a = 4.000 Å, c = 4.124 Å

2θ (°)	d (Å)	I/I_o	hkl
21.80	4.124	11	001
22.30	4.000	13	100
28.15	3.167	3	(ZrO_2)
31.25	2.871	100	101
31.65	2.828	30	110
38.70	2.333	24	111
44.10	2.062	6	002
45.30	2.000	11	200
50.20	1.838	4	102
55.40	1.666	12	112
56.00	1.641	13	211
65.05	1.436	5	202

U. Composition: 70[50:50]-30

Structure: Tetragonal
Parameters: a = 4.022 Å, c = 4.006 Å

2θ (°)	d (Å)	I/I_o	hkl
22.20	4.006	23	001
28.25	3.156	6	(ZrO_2)
31.50	2.838	100	101
38.80	2.319	21	111
45.05	2.011	10	200
50.60	1.793	4	102
55.65	1.638	10	112
56.00	1.641	14	211
65.45	1.419	6	202

V. Composition: 60[50:50]-40

Structure: Rhombohedral

Parameters: $a = 4.017$ Å, $\alpha = 89°53'$ $(1\bar{1}0)$

2θ (°)	d (Å)	I/I_o	hkl
22.20	4.017	20	100
28.35	3.145	6	(ZrO_2)
31.50	2.838	100	$1\bar{1}0$
			$\bar{1}11$
38.85	2.318	18	$1\bar{1}1$
			$11\bar{1}$
45.10	2.008	11	200
50.75	1.797	4	210
56.00	1.640	14	$2\bar{1}1$
			$21\bar{1}$
66.40	1.419	5	$2\bar{2}0$

W. Composition: 50[50:50]-50

Structure: Rhombohedral

Parameters: $a = 3.996$ Å, $\alpha = 89°47'$ (211 and $21\bar{1}$)

2θ (°)	d (A)	I/I_o	hkl
23.30	3.996	27	100
28.40	3.140	6	(ZrO_2)
31.65	2.821	100	$1\bar{1}0$
38.80	2.314	7	111
			$\bar{1}11$
39.00	2.306	16	$1\bar{1}1$
			$11\bar{1}$
45.35	1.998	14	200
51.10	1.789	5	210
56.00	1.636	9	211
56.20	1.630	15	$2\bar{1}1$
			$21\bar{1}$
65.80	1.411	5	$2\bar{2}0$
75.00	1.265	2	310
92.10	1.068	3	$32\bar{1}$

X. Composition: 40[50:50]-60

Structure: Rhombohedral

Parameters: a = 3.984 Å, α = 89°39' (211 and 21$\bar{1}$)

2θ (°)	d (Å)	I/I$_o$	hkl
22.40	3.984	28	100
31.80	2.809	100	1$\bar{1}$0
			$\bar{1}$11
39.20	2.296	18	1$\bar{1}$1
			11$\bar{1}$
45.50	1.992	17	200
51.20	1.786	6	210
56.20	1.634	7	211
56.55	1.625	16	2$\bar{1}$1
			21$\bar{1}$
66.30	1.405	4	2$\bar{2}$0
75.20	1.262	3	310
92.80	1.065	3	32$\bar{1}$

Y. Composition: 20[50:50]-80

Structure: Rhombohedral

Parameters: a = 3.954 Å, α = 89°31' (221 and 22$\bar{1}$)

2θ (°)	d (Å)	I/I$_o$	hkl
22.60	3.954	54	100
27.95	3.190	8	(γ-Bi_2O_3)
28.45	3.135	2	($Bi_2O_3 \cdot 2Fe_2O_3$)
28.95	3.082	2	($Bi_2O_3 \cdot 2Fe_2O_3$)
20.60	2.919	2	(γ-Bi_2O_3)
31.95	2.807	81	110
32.20	2.785	100	1$\bar{1}$0
33.20	2.696	5	(γ-Bi_2O_3)
39.10	2.301	6	111
			$\bar{1}$11
39.60	2.277	25	1$\bar{1}$1
			11$\bar{1}$
45.85	1.977	24	200
51.45	1.774	12	210
51.80	1.763	8	2$\bar{1}$0
56.50	1.625	10	211
57.10	1.612	24	2$\bar{1}$1
			21$\bar{1}$
66.45	1.403	4	220

AA. Composition: 70[30:70]-30

Structure: Tetragonal
Parameters: a = 3.934 Å, c = 4.203 Å

2θ (°)	d (Å)	I/I_o	hkl
21.55	4.203	11	001
22.60	3.934	19	100
28.20	3.162	3	(ZrO_2)
31.35	2.872	100	101
32.15	2.782	33	110
38.95	2.320	30	111
43.75	2.102	6	002
46.10	1.967	13	200
49.70	1.854	5	102
51.35	1.782	4	201
55.20	1.677	11	112
56.65	1.623	18	211
65.20	1.436	7	202
70.00	1.349	4	212
72.45	1.311	2	300
76.00	1.252	4	301
83.45	1.160	3	222
90.10	1.096	3	213

BB. Composition: 60[30:70]-40

Structure: Tetragonal
Parameters: a = 3.914 Å, c = 4.170 Å

2θ (°)	d (Å)	I/I_o	hkl
21.70	4.170	7	001
22.90	3.914	15	100
31.65	2.854	100	101
32.40	2.768	33	110
39.20	2.306	33	111
44.10	2.085	7	002
46.35	1.957	20	200
49.90	1.840	8	102
51.75	1.772	7	201
55.45	1.665	11	112
57.00	1.614	27	211
65.45	1.427	11	202
67.40	1.384	7	220
76.45	1.245	7	301

CC. Composition: 50[30:70]-50

Structure: Tetragonal
Parameters: a = 3.914 Å, c = 4.204 Å

2θ (°)	d (Å)	I/I_o	hkl
21.30	4.204	7	001
22.80	3.914	18	100
28.20	3.162	6	(ZrO_2)
31.30	2.865	100	101
32.35	2.768	37	110
39.00	2.312	40	111
44.00	2.102	4	002
46.35	1.957	16	200
49.20	1.852	5	102
51.30	1.774	5	201
55.00	1.674	6	112
56.95	1.616	22	211
65.30	1.432	4	202

DD. Composition: 40[30:70]-60

Structure: Rhombohedral
Parameters: a = 3.968 Å, α = 89°39' (111 and $11\bar{1}$)

2θ (°)	d (Å)	I/I_o	hkl
22.50	3.968	42	100
31.95	2.798	100	$1\bar{1}0$
39.15	2.303	11	111 $\bar{1}11$
39.40	2.287	25	$1\bar{1}1$ $11\bar{1}$
45.70	1.984	20	200
51.30	1.778	10	210
56.75	1.618	20	$2\bar{1}1$ $21\bar{1}$
66.60	1.399	6	$2\bar{2}0$
75.45	1.257	6	310

EE. Composition: 90[15:85]-10

Structure: Tetragonal
Parameters: a = 3.918 Å, c = 4.178 Å

2θ (°)	d (Å)	I/I$_o$	hkl
21.50	4.178	16	001
22.80	3.918	28	100
31.50	2.858	100	101
32.30	2.770	35	110
39.10	2.309	30	111
43.70	2.089	6	002
46.30	1.959	14	200
49.80	1.843	6	102
51.60	1.774	6	201
52.10	1.752	5	210
55.25	1.668	13	112
56.95	1.616	19	211
65.35	1.429	7	202
67.60	1.385	4	220
70.10	1.343	4	212
71.65	1.315	3	221
72.40	1.306	3	300
76.50	1.247	4	301
80.75	1.188	2	311
83.75	1.154	2	222

FF. Composition: 70[15:85]-30

Structure: Tetragonal
Parameters: a = 3.892 Å, c = 4.163 Å

2θ (°)	d (Å)	I/I$_o$	hkl
21.55	4.163	13	001
23.00	3.892	25	100
31.55	2.943	100	101
32.60	2.752	33	110
39.25	2.296	30	111
43.50	2.082	5	002
46.65	1.946	16	200
49.80	1.835	5	102
51.80	1.763	5	201
52.65	1.741	3	210
55.40	1.660	8	112
57.30	1.606	18	211
65.50	1.422	4	202

FF. (cont.)

2θ (°)	d (Å)	I/I_o	hkl
67.95	1.376	4	220
70.25	1.335	3	212
72.25	1.307	2	221
77.00	1.239	3	301
84.00	1.148	2	222

GG. Composition: 40[15:85]-60

Structure: Tetragonal

Parameters: a = 3.836 Å, c = 4.415 Å

2θ (°)	d (Å)	I/I_o	hkl
20.50	4.415	14	001
23.35	3.836	17	100
31.20	2.896	100	101
32.15	2.712	23	110
33.05	2.708	39	(γ-Bi_2O_3)
39.15	2.311	43	111
47.35	1.918	20	200
57.60	1.599	24	211

HH. Composition: 30[15:85]-70

Structure: Rhombohedral

Parameters: a = 3.942 Å, α = 89°35' (111 and 11$\bar{1}$)

2θ (°)	d (A)	I/I_o	hkl
22.80	3.942	41	100
32.20	2.778	100	1$\bar{1}$0
39.40	2.291	9	111
			$\bar{1}$11
39.70	2.271	30	1$\bar{1}$1
			11$\bar{1}$
46.00	1.971	31	200
51.70	1.768	20	210
56.80	1.618	14	211
57.25	1.607	38	2$\bar{1}$1
			21$\bar{1}$
66.90	1.398	6	220

HH. (cont.)

2θ (°)	d (Å)	I/I_o	hkl
67.25	1.389	8	$2\bar{2}0$
71.35	1.314	5	$22\bar{1}$,300
76.05	1.249	7	$3\bar{1}0$
80.30	1.188	4	$3\bar{1}1$ $31\bar{1}$ $\bar{2}\bar{2}2$
85.10	1.135	5	$2\bar{2}2$ $22\bar{2}$

II. Composition: 90[10:90]-10

Structure: Tetragonal

Parameters: a = 3.882 Å, c = 4.138 Å

2θ (°)	d (Å)	I/I_o	hkl
21.90	4.138	9	001
22.15	3.882	21	100
31.85	2.831	100	101
32.75	2.745	40	110
39.50	2.287	34	111
44.00	2.069	8	002
46.75	1.941	23	200
50.15	1.826	8	102
52.10	1.757	6	201
52.60	1.736	5	210
55.70	1.652	13	112
57.50	1.601	23	211
66.00	1.416	8	202
68.20	1.372	6	220
70.70	1.330	6	212
77.00	1.235	6	301

JJ. Composition: 90[5:95]-10

Structure: Tetragonal

Parameters: a = 3.890 Å, c = 4.160 Å

2θ (°)	d (Å)	I/I_o	hkl
21.65	4.160	10	001
22.95	3.890	28	100
28.50	3.129	3	(ZrO_2)
31.65	2.841	100	101
32.55	2.751	40	110
39.35	2.294	41	111
43.75	2.080	7	002
46.65	1.945	27	200
49.90	1.834	8	102
51.90	1.762	10	201
52.40	1.740	4	210
55.50	1.659	13	112
57.35	1.605	32	211
65.75	1.421	9	202
68.00	1.375	6	220
70.60	1.334	5	212
72.55	1.294	5	300
77.05	1.235	8	301
81.30	1.177	4	311
84.35	1.144	4	222

VITA

Dannie Ray Clarida was born April 3, 1943, in Crab Orchard, Illinois. He attended public schools in Crab Orchard and Harrisburg, Illinois and graduated from Crab Orchard High School in May, 1961.

He enrolled in the Missouri School of Mines and Metallurgy, Rolla, Missouri, in September, 1961, and received the Bachelor of Science degree in Chemical Engineering in August, 1965.

He entered the Graduate School of the University of Missouri at Rolla in September, 1965. He received a National Science Foundation Traineeship for the academic year 1965-66.